Vol. 15, 99–110, January 2004

Dynamic and Regulated Association of Caveolin with Lipid Bodies: Modulation of Lipid Body Motility and Function by a Dominant Negative Mutant[V]

Albert Pol,*† Sally Martin,* Manuel A. Fernandez,† Charles Ferguson,* Amanda Carozzi,* Robert Luetterforst*, Carlos Enrich,† and Robert G. Parton*‡

*Institute for Molecular Bioscience, Centre for Microscopy and Microanalysis, and School of Biomedical Sciences, University of Queensland, Queensland 4072, Australia; and †Departament de Biologia Cel·lular, Institut d'Investigacions Biomèdiques August Pi i Sunyer (IDIBAPS), Facultat de Medicina, Universitat de Barcelona, Barcelona 08036, Spain

Submitted June 6, 2003; Revised July 18, 2003; Accepted September 3, 2003
Monitoring Editor: Jean Gruenberg

Caveolins are a crucial component of caveolae but have also been localized to the Golgi complex, and, under some experimental conditions, to lipid bodies (LBs). The physiological relevance and dynamics of LB association remain unclear. We now show that endogenous caveolin-1 and caveolin-2 redistribute to LBs in lipid loaded A431 and FRT cells. Association with LBs is regulated and reversible; removal of fatty acids causes caveolin to rapidly leave the lipid body. We also show by subcellular fractionation, light and electron microscopy that during the first hours of liver regeneration, caveolins show a dramatic redistribution from the cell surface to the newly formed LBs. At later stages of the regeneration process (when LBs are still abundant), the levels of caveolins in LBs decrease dramatically. As a model system to study association of caveolins with LBs we have used brefeldin A (BFA). BFA causes rapid redistribution of endogenous caveolins to LBs and this association was reversed upon BFA washout. Finally, we have used a dominant negative LB-associated caveolin mutant (cav^{DGV}) to study LB formation and to examine its effect on LB function. We now show that the cav^{DGV} mutant inhibits microtubule-dependent LB motility and blocks the reversal of lipid accumulation in LBs.

INTRODUCTION

Recent studies have reported the presence of caveolins on the surface of intracellular lipid bodies (LBs; Fujimoto *et al.*, 2001; Ostermeyer *et al.*, 2001; Pol *et al.*, 2001). Although LBs are common organelles in the cytoplasm of eukaryotic cells, very little is known about their composition or physiological role (see Londos *et al.*, 1999; Brown, 2001; van Meer, 2001 for a review). Lipid bodies consist of a core of apolar lipids (as triacylglycerol or cholesterol esters) encapsulated by a single monolayer of phospholipids (Tauchi-Sato *et al.*, 2002). Although LB biogenesis is not well understood, it is assumed that the LBs form within the two leaflets of the ER membrane to function as lipid storage sites.

To date, a very limited group of proteins have been shown to associate with LBs; perilipins in adipocytes and steroidogenic tissues (Greenberg *et al.*, 1991), adipophilin in most mammalian cells (Heid *et al.*, 1998), oleosins in plants (Qu and Huang, 1990), eicosanoid synthesizing enzymes in various types of cells (Weller and Dvorak, 1994), vimentin (Franke *et al.*, 1987), "capsular proteins" in adrenal cells (Wang and Fong, 1995), and more recently, caveolins (Fujimoto *et al.*, 2001; Ostermeyer *et al.*, 2001; Pol *et al.*, 2001). Although the LB targeting domain of some of these proteins has been examined, a consensus sequence or molecular determinant involved in LB association has not been described.

Caveolins represent an intriguing system to study how membrane components can associate with LBs. Fujimoto and colleagues (Fujimoto *et al.*, 2001) demonstrated that overexpressed caveolin-2 can be partially targeted to LBs. In addition, Ostermeyer *et al.* (2001) showed that caveolin-1 accumulates in LBs when it is linked to an ER-retrieval sequence (cav-KKSL). These studies also demonstrated that caveolins can be artificially directed into LBs when the functional integrity of the Golgi complex is disrupted by means of brefeldin A (BFA). It was suggested that the presence of caveolin in LBs is more artifactual than physiological, a consequence of the accumulation of high levels of caveolins in the ER. This was supported by the fact that endogenous caveolins were not detected on the LBs and because the transfected caveolins could not exit the LBs when cells were allowed to recover BFA. Using a different strategy, we have previously demonstrated (Pol *et al.*, 2001) that a mutant caveolin protein (cav3^{DGV}) that acts as a dominant negative for caveolin function accumulates irreversibly in the LBs.

Article published online ahead of print. Mol. Biol. Cell 10.1091/mbc.E03–06–0368. Article and publication date are available at www.molbiolcell.org/cgi/doi/10.1091/mbc.E03–06–0368.

[V] Online version of this article contains video material for some figures. Online version is available at www.molbiolcell.org.

‡ Corresponding author. E-mail address: R.Parton@imb.uq.edu.au.

Abbreviations used: BFA, brefeldin A; BHK, baby hamster kidney cells; Cav^{DGV}, caveolin 3 DGV truncation; CyHx, cyclohexamide; DAPI, 4′,6-diamidino-2-phenylindole dihydrochlorid; ER, endoplasmic reticulum; FRT, Fisher rat tyroid cells; GFP, green fluorescent protein; LB, lipid body; OlAc, oleic acid; PM, plasma membrane; PH, partial hepatectomy; YFP, yellow fluorescent protein.

Supplemental Material can be found at: http://www.molbiolcell.org/content/suppl/2003/10/03/E03-06-0368.DC1.html

Table 1. Antibodies used in this work

Antibody	Abbreviation	Reference
Monoclonal mouse anti–caveolin-1	moZy	Zymed Labs. 03-6000
Monoclonal mouse anti–caveolin-1	moTL	Transduction Labs. C13620
Monoclonal mouse anti–caveolin-2	TLcav2	Transduction Labs. C57820
Rabbit polyclonal anti-caveolin (N-terminal domain)	rbTL	Transduction Labs. C13630
Rabbit affinity purified anti-caveolin (caveolin identity domain)	Con-cav	Luetterforst *et al.* (1999)
Monoclonal mouse anti-GM130	GM130	Transduction Labs. G65120
Monoclonal mouse anti-adipophilin	Adipophilin	Progen 651102

The fact that this mutant causes an intracellular cholesterol imbalance suggested a possible role for caveolin in intracellular lipid transport from these organelles (Pol *et al.*, 2001; van Meer, 2001). Although caveolin is an integral membrane "hairpin"-like protein, it has also been suggested that caveolin may function without being integrated in a membrane (Uittenbogaard *et al.*, 1998, 2002). Whether a cytosolic intermediate could be involved in trafficking to lipid bodies remains unknown. It has been postulated that because caveolins have a single central hydrophobic domain similar to oleosins this hydrophobic domain may interact with the core of neutral lipids in the LBs.

In the present study, we have addressed whether caveolins associate with LBs under physiological conditions and, if so, whether this is a regulated process. We demonstrate that endogenous caveolins can move in and out of the LB, in a bidirectional process, suggesting that specific retrieval mechanisms must exist. We also prove that endogenous caveolin moves to the LBs not only after disrupting the Golgi membranes with BFA, but also in response to the intracellular accumulation of lipids. In regenerating liver caveolin relocates from the plasma membrane to newly formed LBs, suggesting a role for caveolin in lipid transport to or from the LBs. Finally, we have investigated the effect of a caveolin dominant negative mutant on LB function and show that specific effects on LBs can underlie the perturbation of lipid regulation and signal transduction at the cell surface.

MATERIALS AND METHODS

Plasmids, Antibodies, and Reagents

YFP-tagged full-length cav3 and YFP-tagged and GFP-tagged cav3^{DGV} were generated following the method described previously (Luetterforst *et al.*, 1999). Primary antibodies and their abbreviations used in this work are summarized in Table 1. Gold-conjugated protein A was purchased from the University of Utrecht, Utrecht, The Netherlands. Fluorescein, Cy3, and gold-conjugated secondary antibodies were from Jackson ImmunoResearch (West Grove, PA). HRP-conjugated secondary antibodies were from Zymed Laboratories (South San Francisco, CA). BFA), cycloheximide (CyHx), oil red, and nocodazole were purchased from Sigma Chemical Co. (St. Louis, MO) 4′,6-diamidino-2-phenylindole dihydrochloride (DAPI) and Nile red were from Molecular Probes (Eugene, OR). Oleic acid (OlAc) and fatty acid free BSA were from Calbiochem (La Jolla, CA).

Cell Culture

Baby hamster kidney cells (BHK), Fisher rat thyroid cells (FRT), Vero cells, and A431 cells were maintained in DMEM with 10% vol/vol serum supreme (SS; Biowhitaker, Walkersville, MD) supplemented with 2 mM L-glutamine, penicillin (50 U/ml), and streptomycin sulfate (50 μg/ml) and in some experiments supplemented with 50 μg/ml oleic acid and free fatty acid BSA. Cells were split the day before the experiment or transfection. Cells were transfected using Lipofectamine plus (Invitrogen, San Diego, CA) as outlined previously (Pol *et al.*, 2001).

Immunofluorescence Microscopy, Electron Microscopy, and Time-Lapse Video Microscopy

Immunofluorescence, videomicroscopy and immunoelectron microscopy on frozen sections was performed as described previously (Pol *et al.*, 2001). Nile red was diluted in the mounting mowiol (1/1000 from a stock saturated solution in acetone) and for cells were fixed in PFA for oil red cells were incubated 1 min on ice cold (a saturated and filtered stock solution in 50% Isopropanol). Immunolabeling of fractions was performed by mixing fractions in a 1:1 vol/vol ratio with 8% PFA in PBS at room temperature and applied to polylysine-coated grids. The grids were then washed with PBS, labeled, and embedded in methylcellulose/uranyl acetate as for frozen sections. For quantitation of LB motility, cells were transfected with cav3^{DGV}-YFP or caveolin-3-YFP. After 24 h, expressing cells were identified by fluorescence microscopy, and LB motility in those cells was assessed under bright field illumination. To track the movement of individual LBs a composite was made in Photoshop (Adobe Systems, San Jose, CA) from three images taken at intervals of 10 s (with each image colored differently). The total distance moved was then measured in NIH image (Bethesda, MD).

Cell Fractionation and Western Blot

Confluent 10-cm dishes of BHK cells were washed twice with cold PBS before being scraped into ice-cold 10 mM Tris, pH 7.5, 150 mM NaCl, 5 mM EDTA, and a mixture of protease and phosphatase inhibitors. Cells were homogenized by gentle sonication for 10 s on ice and by passage through a 22-gauge needle 10 times at 4°C. Nuclei and unbroken cells were removed by centrifugation at 5000 rpm for 5 min at 4°C in a TLS-55 rotor (Beckman, Fullerton, CA). The resulting supernatant was mixed with the same volume of 2.5 M sucrose and loaded at the bottom of a discontinuous sucrose gradient composed by seven phases ranging from 5 to 35% (wt/vol) sucrose. The tubes were centrifuged at 50,000 rpm for 4 h at 4°C in a TLS-55 rotor (Beckman). Finally, 14 aliquots were unloaded from the top of the gradient and stored at −20°C. When the isolated fractions were analyzed for electron microscopy, the top fraction of the gradient (fraction 1) was processed immediately. For Western blotting analysis with a polyclonal anticaveolin antibody (rbTL), equal volumes of each aliquot were electrophoretically separated by SDS-PAGE in 12% polyacrylamide gels as described previously (Pol *et al.*, 2001). The quantification of Western blots was calculated densitometrically with the Bio-Image (Millipore, Bedford, MA) program that reads and calculates the band intensity and the band area. In Figures 2, B and F, and 4B, the results are expressed as percentages of every band compared with the total integrated intensity. In Figure 4, E–G, the results are expressed as percentages of every band compared with the integrated intensity corresponding to the first lane of the blot. Only bands in the same gel were compared, but the final percentage corresponds to the mean of at least three different experiments.

Liver Regeneration Studies

Male Sprague Dawley rats weighing 200–220 g were used for all experiments. Animals were kept under a controlled lighting schedule with a 12-h dark period. All animals received human care in compliance with institutional guidelines regulated by the European Community. Food and water were available ad libitum but rats were fasted overnight before experiments. Partial hepatectomies (PHs) were carried out according the procedure of Higgins and Anderson (1931), in which 66% (medial and left lateral lobes) of liver mass is removed under Fluorane anesthesia. Hepatocytes were isolated and cultured from a young male Sprague Dawley rat using a sterile method (Bissell *et al.*, 1973) as described previously (Calvo *et al.*, 2001). Crude membranes, endosomes, and CEF were obtained as described previously (Pol *et al.*, 1999).

RESULTS

Endogenous Caveolins Associate with Lipid Bodies: Identification of Caveolins on LBs in Lipid-loaded A431 and FRT Cells

The visualization of overexpressed caveolins and mutant caveolins associated with LBs suggest that caveolins have some propensity to associate with LBs. However, endogenous caveolins have not been observed in LBs in the absence

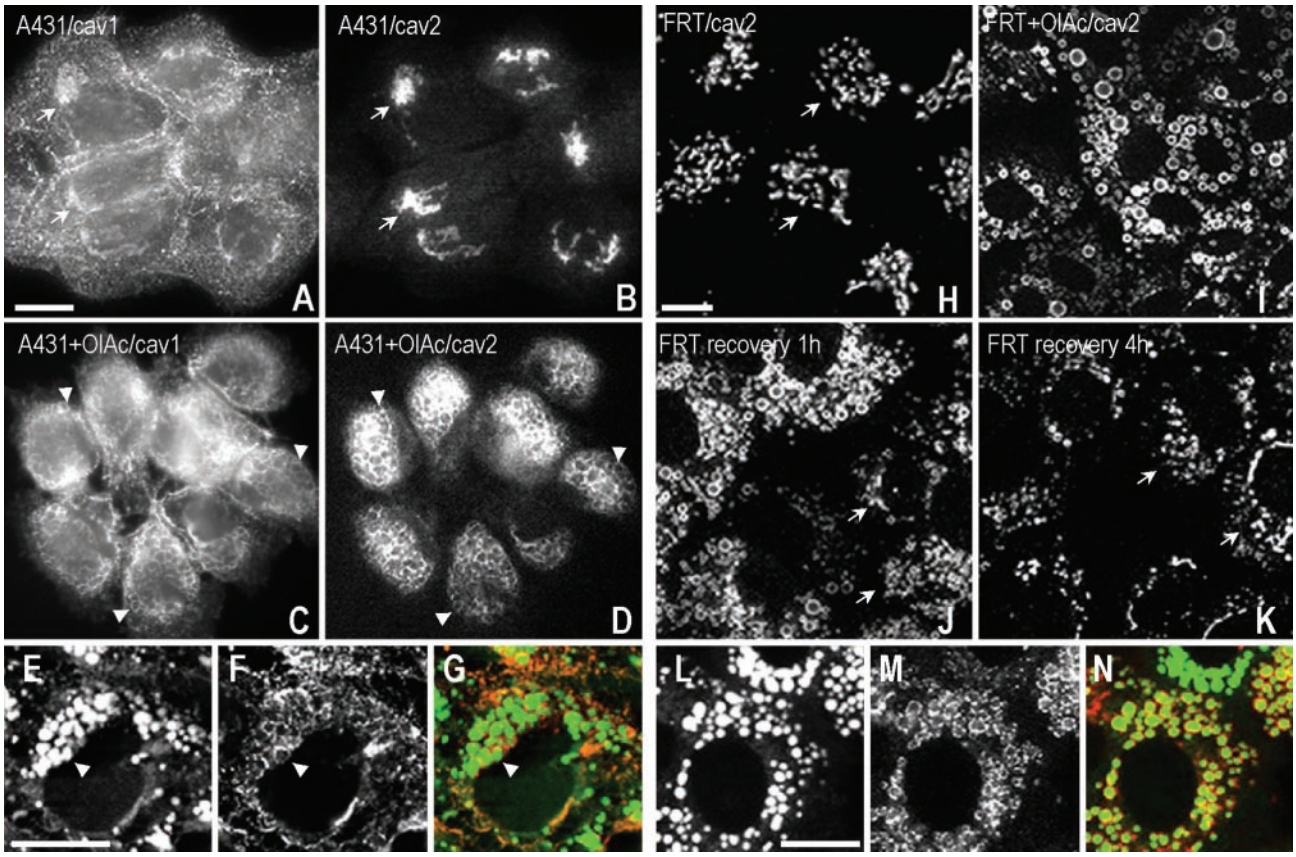

Figure 1. Caveolins traffic between LBs and the Golgi complex in response to lipid loading of the cells. (A–G) A431 cells were incubated with or without 50 μg/ml OlAc for 24 h and labeled with specific caveolin-1 (rbTL) and caveolin-2 (TLcav2) antibodies. In untreated A431 cells, caveolin was located on the plasma membrane and the Golgi complex (A). In contrast, caveolin-2 was accumulated in the Golgi complex (B). Both caveolins showed a high degree of colocalization in the Golgi complex (arrows). In contrast, lipid loading caused redistribution of caveolin-1 (C) and 2 (D) to ring-shaped cytoplasmic structures (arrowheads) identified as lipid bodies by Nile red staining (E–G). Some LBs contained both caveolins (arrowheads). (H–N) FRT cells were incubated for 16 h with OlAc and labeled with specific anticaveolin-2 (TLcav2) antibodies. In untreated cells, caveolin-2 was concentrated in the Golgi complex (H). In the presence of OlAc (I), caveolin-2 redistributed to Nile red–positive lipid bodies (L–N). In addition, a loss of Golgi staining for caveolin-2 was apparent. When OlAc was washed out, caveolin-2 partially recovered its initial distribution in the Golgi complex after 1 h (arrows in J). The recovery was completed 4 h after of the washout (K). Bars, 5 μm.

of BFA and the trafficking pathways to and from LBs have not been defined. We investigated whether endogenous caveolins could associate with LBs under physiological conditions and specifically whether this might occur in response to lipid loading of cells. We therefore investigated whether caveolins associate with LBs in A431 cells and FRT cells grown in the presence of elevated levels of the free fatty acid, oleic acid.

A431 cells have abundant caveolae (Parton, 1994) and show strong staining for caveolin-1 (rbTL) in the Golgi complex and at the cell surface (Figure 1A). In contrast, caveolin-2 (TLcav2) only shows labeling in the Golgi complex in these cells (arrows, Figure 1B). Treatment of cells for 24 h with oleic acid (OlAc) caused redistribution of caveolins 1 and 2 to ring-shaped cytoplasmic structures (arrowheads, Figure 1, C and D) identified as LBs by the colocalization with the neutral lipid stain, Nile red (Figure 1G). Association of caveolins with the LBs was accompanied by an apparent decrease in staining at the PM for caveolin-1 and partial loss of Golgi staining for caveolin-2. FRT cells lack caveolin-1 but show strong Golgi labeling for caveolin-2 (TLcav2; arrows, Figure 1H). We investigated whether in the absence of caveolin-1, caveolin-2 could redistribute to LBs. As shown in Figure 1I, treatment of cells with OlAc caused almost complete redistribution of caveolin-2 from the Golgi complex to LBs, which colabeled for Nile red (Figure 1N).

To investigate the reversibility of the association of caveolins with the LBs, OlAc was subsequently removed from the culture medium. Caveolin-1 and -2 in A431 cells (unpublished data) or caveolin-2 in FRT cells (Figure 1K) rapidly redistributed from the LBs to the Golgi complex. Labeling for caveolin-2 reappeared within the Golgi complex after 1 h of removing the OlAc (arrows, Figure 1J). The recovery was completed within 4 h (Figure 1K). The recovery of caveolin occurred before there was any significant decrease in size or number of LBs in the cells and before loss of staining for the lipid body protein, adipophilin (unpublished data). Therefore, caveolin-1 and -2 show rapid and reversible association with LBs. These studies identify a bidirectional trafficking pathway between LBs and the Golgi complex, which is controlled by lipid loading of the cells.

Caveolins Associate with LBs in Regenerating Liver

The accumulation of LBs in the early stages of liver regeneration after partial hepatectomy (PH, removal of 66% of the

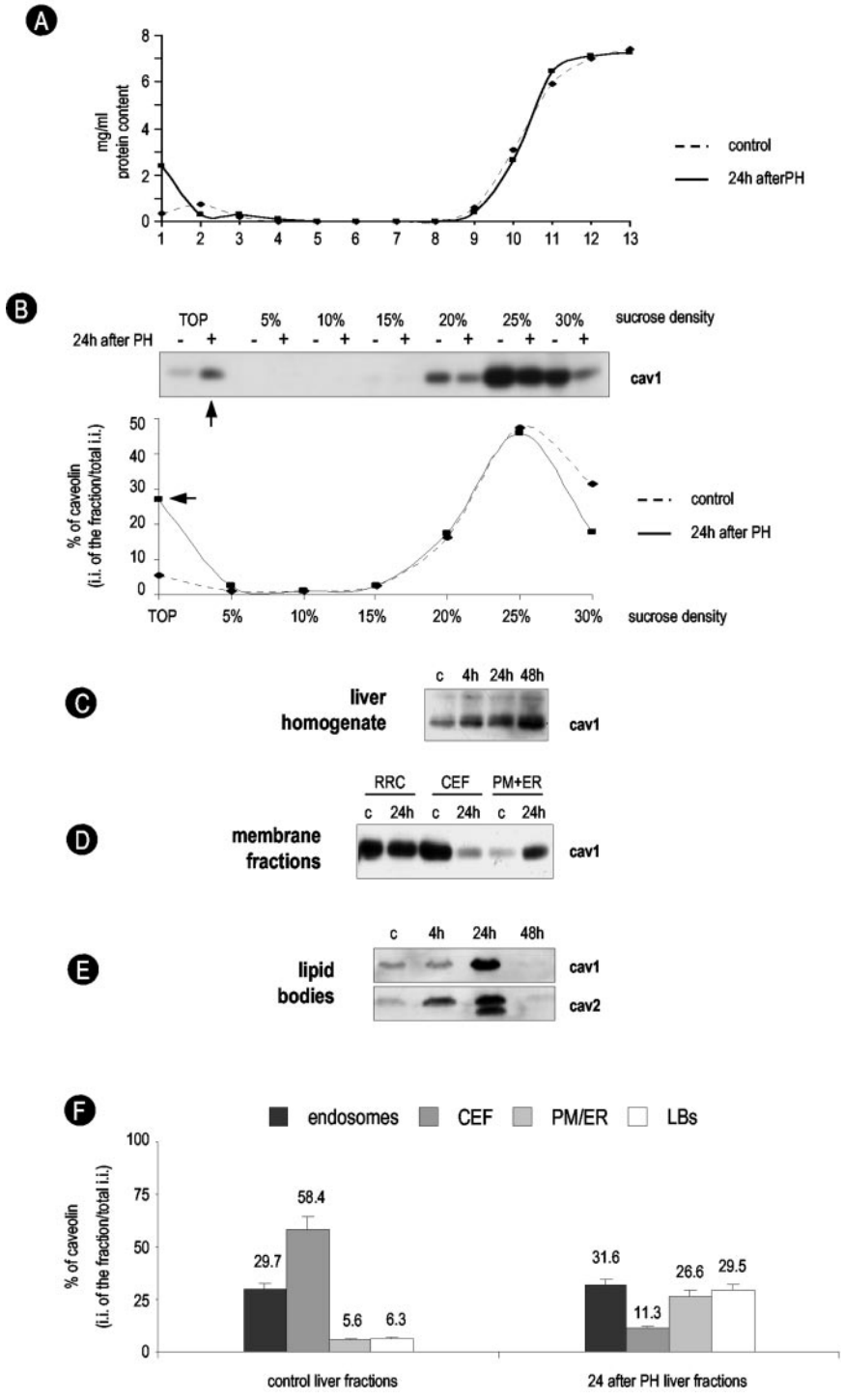

Figure 2. Caveolin associates with LBs during rat liver regeneration. Biochemical characterization. (A) Amount of protein and distribution of caveolin in sucrose density gradients of liver postnuclear supernatants. Twenty-four hours after PH there is a significant redistribution of caveolin to LBs (top of the gradient, arrow). (B) Quantification by densitometry of caveolin distribution (shown in A) in control or in livers 24 h after PH. The results are expressed as the level of caveolin in each lane relative to the total intensity. Quantification was performed from the data in the figure but similar results were obtained in three independent experiments. Twenty-four hours after the partial hepatectomy 26.86% of the total caveolin can be found in LBs (arrow). (C–E) At different times after a partial hepatectomy (PH), the amount of caveolin present in liver homogenates and in different subcellular fractions (RRC; recycling receptor endosomes, CEF; caveolae-enriched plasma membrane fraction, and PM/ER; crude membrane fraction containing PM and ER membranes) was compared by Western blotting (rbTL). (C) Total levels of caveolin in the liver increases after PH. (D) Caveolin redistributes from the caveolae-enriched fraction (CEF) to the crude membrane fraction containing the ER and plasma membrane. (E) An LB-enriched fraction was isolated from control and regenerating livers and the amount of caveolin-1 (rbTL) and -2 (TLcav2) analyzed by Western blot. While the amount of caveolins in control livers was relatively low, both caveolins accumulated in the LB fraction 24 h after PH. At later stages of regeneration (48 h) the levels of caveolins in LBs decreased. (F) The redistribution of caveolin in the purified membrane fractions, described in D and E, was quantified by densitometry as described previously.

liver mass) has been well documented (Glende and Morgan, 1968; see also Figure 3). This offers an excellent physiological system to examine formation and association of proteins with LBs in vivo.

We first analyzed the distribution of caveolin in sucrose density gradients of liver postnuclear supernatants. As shown in Figure 2, A and B, there was a significant redistribution of caveolin from the bottom of the gradient in control livers to accumulate in a very low density fraction in regenerating liver 24 h after PH (26.86% of the total caveolin). To gain insights into the redistribution of caveolin, we analyzed the levels of caveolin-1 in different subcellular membrane fractions isolated from control and regenerating rat liver. After PH, there was a progressive increase in the levels of caveolin in the homogenates (Figure 2C). In parallel, the amount of caveolin-1 in a crude membrane fraction (composed mainly of PM and ER membranes) increased at 24 h of the regenerative process (from 5.6% of the total caveolin in control liver to 26.6% 24 h after PH; Figure 2, D and F). Interestingly, although the amount of caveolin associated

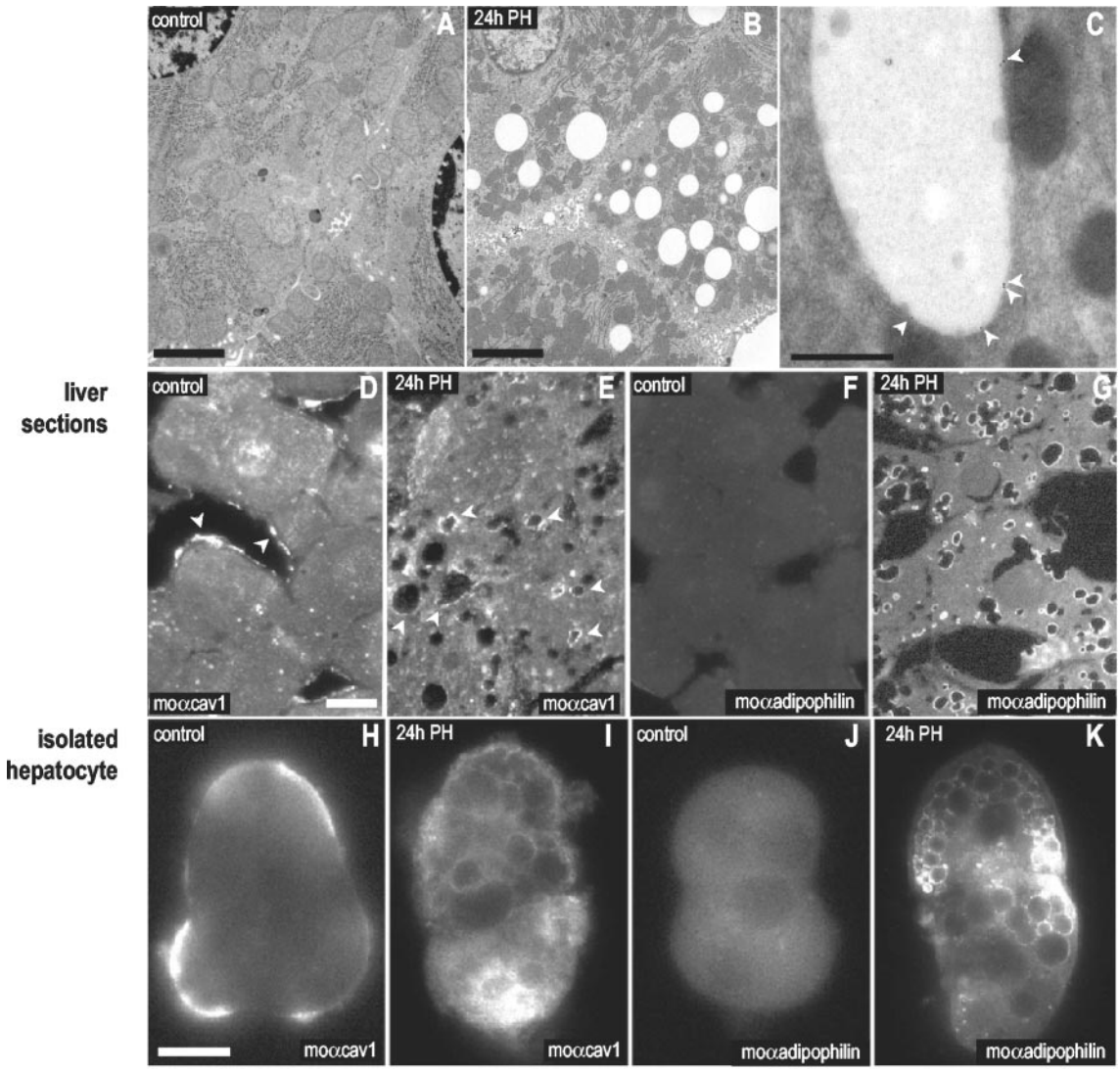

Figure 3. Caveolin associates with LBs during rat liver regeneration. Microscopic characterization. Spur sections of control livers (A) and livers 24 h after PH (B). The accumulation of LBs in the cytosol of the hepatocytes can be observed. (D–G) Sections of control (D and F) and regenerating livers (E and G) were labeled with a mAb for caveolin-1 (moTL; D and E) and with a specific antibody to adipophilin (a marker of LBs; F and G). After 24 h of PH caveolin relocated from the sinusoidal PM of the hepatocytes (arrows) to intracellular structures identified as LBs by the presence of adipophilin. This was confirmed by immunogold electron microscopy on frozen sections using the rbTL antibody (C). (H–K) Hepatocytes from control (H and J) or regenerating livers (I and K) were isolated and the distribution of caveolin analyzed with a mAb for caveolin-1 (moTL; H and I) and for adipophilin (J and K). As in liver sections, 24 h after a PH caveolin-1 was detected decorating the surface of intracellular LBs. Bars, (A and B) 2 μm; (D) 200 nm; (E–L) 5 μm.

with the endosomes of the receptor recycling compartment (RRC; Pol *et al.*, 1999) was not modified after PH, the levels of caveolin in a caveolae-enriched plasma membrane fraction (CEF) decreased significantly (from 58 to 11.3%; Figure 2, D and F) suggesting redistribution of the protein from the PM to an intracellular compartment.

To investigate whether caveolin-1 and -2 associate with LBs, we isolated LBs at different times of the regeneration process by flotation in sucrose density gradients. LBs accumulate at the top of the gradient due to their low density (see MATERIALS AND METHODS for more details and see Figure 4 for the characterization of the gradients). Figure 2D shows that although the amount of caveolin-1 and -2 in the LB fraction from control liver was low, both caveolins accumulated in LBs 24 h after PH (29.5% of the total caveolin accumulated in LBs; Figure 2, E and F). Interestingly, at later stages of regeneration (48 h), when LBs are still abundant (unpublished data), the levels of caveolins in this fraction decreased dramatically, suggesting regulated redistribution from the LBs.

We finally analyzed by means of microscopy techniques the reorganization of caveolin in response to the regeneration process. Figure 3, A and B, shows the high concentration of LBs in the cytosol of hepatocytes 24 h after PH. Next, we studied the distribution of caveolin-1 (moTL) by immunofluorescence microscopy on sections from control and regenerating livers 24 h after PH. In control liver, caveolin was almost exclusively associated with the PM, corresponding to the sinusoidal region of hepatocytes (arrowheads, Figure 3D). However, after 24 h of PH there was a clear redistribution of caveolin to the LBs (arrowheads, Figure 3E) and this could be confirmed by immunoelectron microscopy

on ultrathin frozen sections (Figure 3C). The relocation of caveolin-1 contrasted with the immunofluorescence pattern of ASGP-R, a well-characterized plasma membrane receptor located in clathrin-coated pits, which did not alter after PH (unpublished data). Adipophilin, a marker of LBs, accumulated in the LBs formed 24 h after PH (Figure 3G). We further analyzed the relocation of caveolin during the regeneration process in isolated hepatocytes. As previously observed in liver sections, and in contrast to control hepatocytes (Figure 3H), caveolin (moTL) decorated the surface of spherical structures of the regenerating hepatocytes (Figure 3I), which were identified as LBs by labeling for adipophilin (Figure 3K).

In summary, the distribution of caveolin in the hepatocyte undergoes a significant change during the first hours of the regeneration process. After 24 h of PH caveolin relocates from the PM to intracellular LBs, suggesting a role for caveolin in lipid homeostasis.

BFA Causes Redistribution of Caveolin to LBs: A Model System to Follow Caveolin Accumulation in LB

It has been shown that heterologously expressed caveolin can redistribute to LBs when the Golgi integrity is disrupted by means of BFA and this offers an excellent model system to further investigate trafficking of caveolin to and from LBs.

We studied the kinetics of association and the reversibility of the redistribution of caveolin to LBs in BHK cells. As shown by the con-cav antibody (an antibody that exclusively recognizes the intracellular pool of caveolin (Figure 4A; Pol *et al.*, 2001) after 2 h with the drug caveolin accumulated in the periphery of the rings identified as LBs (arrows, Figure 4B) by the presence of adipophilin (unpublished data). To test the reversibility of the BFA effect on caveolin, the cells were treated with BFA, and then the drug washed out, allowing the cells to recover for 30 min. The recovery after the washout was almost complete (Figure 4C).

To confirm the results obtained by immunofluorescence, we further characterized by biochemical methods, the association of caveolin with purified LBs. To induce the formation of LBs the cells were also treated with OlAc as previously described in Figure 1. Then, control or OlAc-treated BHK cells were treated with BFA, and the cell homogenates were resolved on sucrose density gradients by ultracentrifugation. In this gradient, ER, Golgi, and PM markers were detected around 25% sucrose, and adipophilin was detected around 5% sucrose (unpublished data). As expected, in untreated cells, caveolin (rbTL) accumulated in densities corresponding to the PM (25% sucrose, fraction 6–7) and little (0.3% of the total caveolin) was detected at the density corresponding to the LBs (5% sucrose, fraction 1; Figure 4D, top panel). The enrichment of LBs and purity of this fraction was confirmed by electron microscopy (see later in Figure 5A). When cells treated with BFA or with OlAc were resolved by the same method, a significant amount of caveolin shifted to fraction 1 (Figure 4D, middle panel). The accumulation of caveolin at the top of the gradient was maximal (6.8% of the total caveolin) when cells preincubated in OlAc were treated for 2 h with BFA (Figure 4D, bottom panel). Note that although the amount of caveolin in top of the gradient increases considerably (~20-fold), it still represents a low percentage of the total cellular caveolin.

To quantify the amount of caveolin present on LBs in response to the different treatments, equal volumes of fraction 1 were analyzed by Western blotting with the rbTL antibody (Figure 4E) and quantified by densitometry. As compared with control cells, 2.99 times more caveolin was detected in the fraction 1 isolated from cells treated with BFA, 4.99 times when the cells were treated with OlAc, and 15.14 times when cells preincubated in OlAc were treated with BFA. The same protocol was used to monitor the time course of the accumulation of caveolin in fraction 1 in response to BFA. As shown previously by immunofluorescence, there was a peak of caveolin (2.98 times) in fraction 1 corresponding to cells treated for 2 h with the drug (Figure 4F, left panel). The amount of caveolin decreased at longer times (1.63 times). However, when the cells were pretreated with OlAc and then incubated with BFA, caveolin rapidly accumulated on LBs (2.19 times after 1 h; Figure 4F, right panel). In this case, the high levels of caveolin detected in fraction 1 were prolonged even after 4 h of incubation (4.55 times). Finally, the cells were treated for 2 h with BFA and then the drug washed out for different times. In accordance with the immunofluorescence results, in control cells the amount of caveolin in LBs returned to control levels 30 min after the washout (Figure 4G, left panel) or close to control levels 45 min after the washout in cells pretreated with OlAc (Figure 4G, right panel).

Immunolabeling of fraction 1 by electron microscopy confirmed the association of caveolin with the LBs and allowed quantitation of the level of caveolin per LBs. Analysis of fractions from OlAc-treated cells, OlAc/BFA-treated cells (Figure 5C), or OlAc/BFA-treated cells allowed to recover for 30 min (Figure 5D) showed 42 ($\pm$27), 152 ($\pm$106; however, with 80% of the LBs ranging from 95 to 222), and 42 ($\pm$31) gold particles, respectively. In addition, the OlAc-treated cells were processed for frozen sectioning and immunolabeled with anti–con-cav antibodies. Specific labeling was associated with electron lucent LBs (Figure 5B).

Therefore, the treatment with BFA offers an excellent in vitro model to induce a rapid but reversible association of caveolins with LBs. This system can now be used to study the mechanisms involved in the recruitment of membrane proteins to these organelles. The results obtained in lipid loaded cells also confirm that the steady state levels of caveolin in this organelle are modulated by the lipid content or size of the LBs.

A Caveolin Dominant Negative Mutant Affects LB Motility and Lipid Redistribution

Caveolin-3 DGV (cav^{DGV}) has been shown to perturb plasma membrane lipid raft domains through an indirect effect on cellular cholesterol. The mutant protein accumulates irreversibly on LBs and causes increased accumulation of neutral lipids in this organelle, while decreasing plasma membrane free cholesterol. We investigated the effect of the irreversible association of the cav^{DGV} protein on the formation of LBs and on their properties.

LBs have been shown to undergo microtubule-dependent motility. The dynamic behavior of LBs was monitored by time-lapse video microscopy. LBs were stained with Nile red and then followed by bright field microscopy for 3 min. LBs showed bidirectional saltatory movements (see 3 representative trajectories in Figure 6A, and complete movie in supplementary material), which although far less extensive than those observed in the same cells for late endosomes, are completely blocked by incubation with nocodazole (unpublished data). In striking contrast, transfection with cav^{DGV}-YFP caused an almost complete block in LB motility (see yellow arrows in Figure 6A) compared with cells expressing cav-3-YFP (0.2 ± 0.07 vs. 1.1 ± 0.2 μm/s). Thus one effect of cav^{DGV} is to decrease LB motility.

One possibility to explain the inhibitory effects of cav^{DGV} is that the mutant is affecting the correct formation of LB, or, alternatively, that cav^{DGV} can form aberrant LBs indepen-

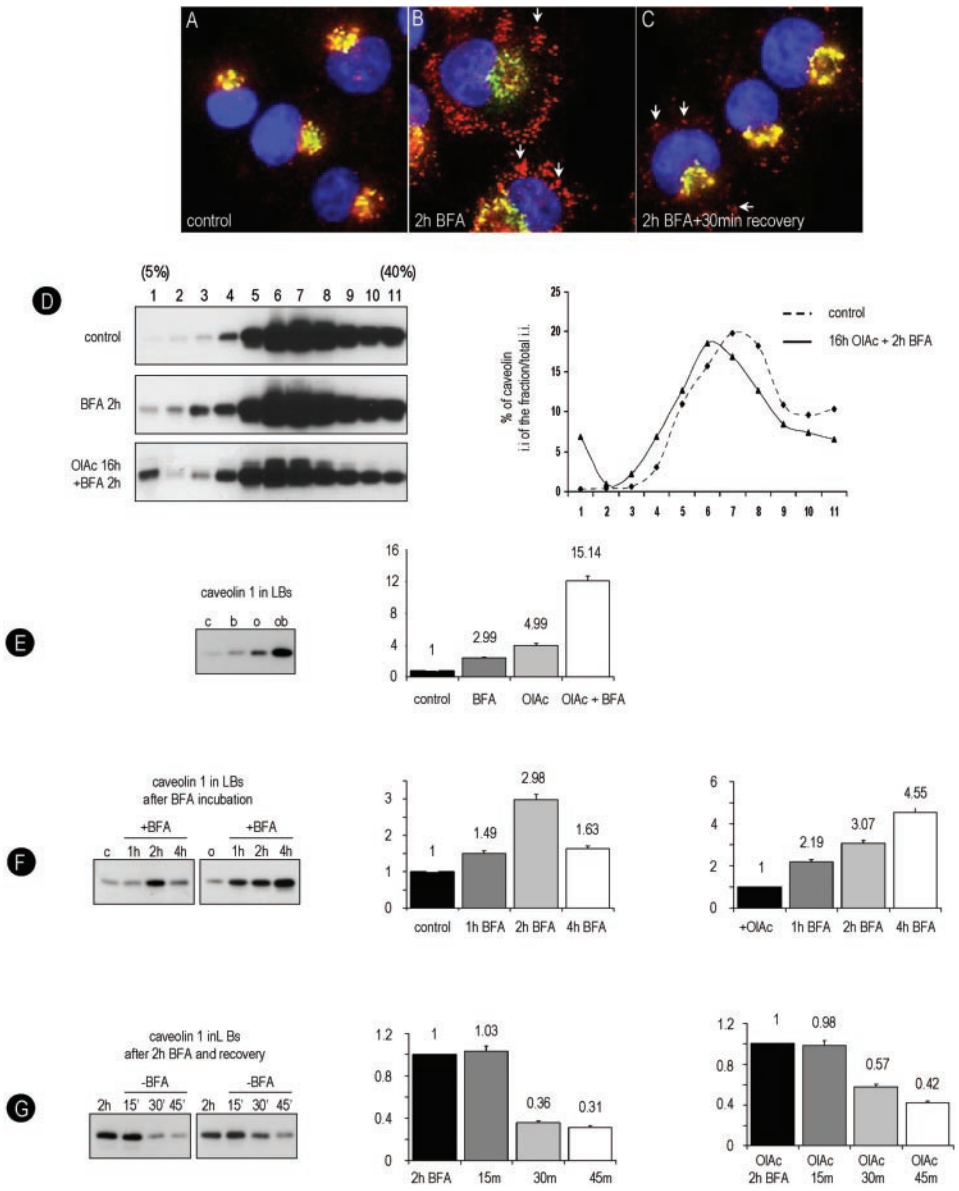

Figure 4. BFA causes redistribution of caveolin to LBs; a model system to follow caveolin accumulation in LB. (A–C) Control BHK cells were treated for 2 h with 5 μg/ml BFA. Caveolin distribution was analyzed with the con-cav antibody (red channel) in combination with GM130 (a Golgi marker, green channel) and DAPI (nuclei, blue). Caveolin is detected in LBs (arrows in B). When, after 2 h with BFA, the drug is washed out for 30 min, the recovery is almost complete (arrows C). (D–G) Untreated or OlAc-treated BHK cells were incubated for 2 h with 5 μg/ml BFA and then resolved on sucrose density gradients. (D) In control cells caveolin (rbTL) accumulates in densities corresponding to the PM (fraction 6–7, 20% sucrose; top). Caveolin partially shifts to the top of the gradient (fraction 1) when the cells are preincubated with 50 μg/ml OlAc or treated for 2 h with BFA (middle). The accumulation in the top of the gradient is maximal (6.8%) when cells pretreated with OlAc are incubated with BFA (bottom). Quantification, as described for Figure 2B, was performed from the data in the figure but similar results were obtained in three independent experiments. (E) The LB fraction (1) for each treatment were isolated in parallel and equal volumes resolved by Western blotting. The levels of caveolin after the different treatments (shown in the histograms) was quantified by densitometry and it is indicated as relative to the first lane. (F) Using the same method, we compared the amount of caveolin in fraction 1 corresponding to the gradients from cells treated for different times with BFA, in either 10%SS (left panel) or OlAc-pretreated cells (right panel). In control cells caveolin reaches a peak after 2 h with the drug; however, in OlAc-treated cells high levels of caveolin are sustained after 4 h with BFA. (G) BHK cells were treated for 2 h with BFA and then the drug was washed out for different times. In fraction 1 of control (left panel) or in cells pretreated with OlAc (right panel), the levels of caveolin return to the initial levels after 30 or 45 min, respectively.

dently of the presence of lipids. Therefore cav^{DGV}-YFP was transfected into serum-starved cells that lack LBs as defined by Nile red staining and by bright field microscopy. In contrast to full-length caveolin (unpublished data), cav^{DGV} localized to an extensive reticular compartment identifiable as the ER with no punctate labeling evident (Figure 6B, time 0). Addition of OlAc to the starved cells caused an extremely rapid formation of distinct puncta, putative forming LBs, within minutes (Figure 6B, and complete movie in supplementary material). At high magnification can be observed that cav^{DGV} accumulates in the periphery of the forming LBs (unpublished data). Thus OlAc addition causes cav^{DGV} to

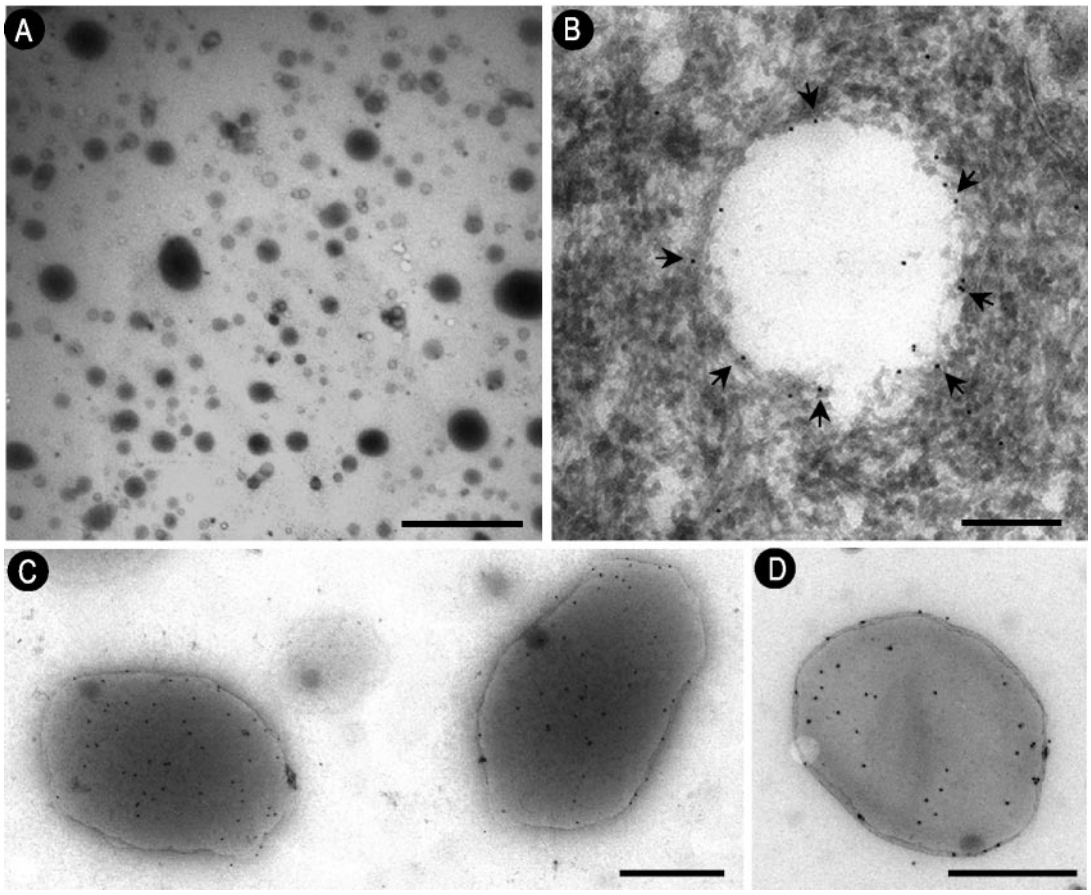

Figure 5. BFA causes redistribution of caveolin to LBs; microscopic characterization. (B) OlAc-treated cells were processed for frozen sectioning and immunolabeled with anti–con-cav antibodies. Specific labeling is associated with electron lucent LBs. (A, C, and D) Fraction 1 was applied to an EM grid and immunolabeled (without sectioning). (A) A low-magnification overview demonstrating the purity of the fraction. (C and D) Immunolabeling with the con-cav antibody of fraction 1 from OlAc and BFA-treated cells (C) and the cells after 30 min of recovery (D). Bars, 200 nm.

redistribute from its diffuse distribution within the ER to distinct sites involved in LB formation. Cav^{DGV} can therefore be used as a marker to follow LB biogenesis, and these experiments illustrate the extremely rapid dynamics of LB formation.

Previous studies showed that cav^{DGV} expression increases neutral lipid accumulation in LBs (Pol *et al.*, 2001). Although the intracellular accumulation of lipids induced by cavDGV was variable, the mean increase in oil red staining in cavDGV-transfected cells was more than twofold higher than nontransfected cells (pixel intensity cavDGV-transfected/untransfected cells 2.70/1.23; Figure 7E). To examine the effect of cav^{DGV} expression in detail, we next investigated whether OlAc, which diffuses into the cell bypassing the endosomal system, is accumulated more rapidly in LBs in cav^{DGV}-expressing cells. At early times (2 h) of OlAc addition we observed no significant differences in neutral lipid staining of cav^{DGV}-transfected cells compared with untransfected cells (unpublished data). After an incubation of 16 h with OlAc, all the cells contained characteristic enlarged LBs (pixel intensity: 6.25/5.72; compare Figure 7A with Figure 7B). We then investigated whether cav^{DGV} expression affected the handling of accumulated neutral lipids after removal of OlAc from the culture medium. Untransfected cells showed a progressive reduction in neutral lipid staining upon removal of OlAc. However, there was a significant delay in the loss of neutral lipid staining in the cav^{DGV}-expressing cells (Figure 7C; pixel intensity: 5.29/2.25). Although LBs of untransfected cells became smaller, the LBs containing cav^{DGV} maintained their original size. The differences were more obvious 24 h after the washout, when only the cav^{DGV} cells contained the enlarged LBs (compare Figure 7A with Figure 7D; pixel intensity: 5.41/1.36). Thus the cav^{DGV} mutant has an inhibitory effect on the catabolism/redistribution of lipids out of lipid bodies.

In conclusion, we have shown that the cav^{DGV} mutant associates rapidly with LBs upon OlAc treatment of cells and we have revealed a striking effect of the mutant protein on LB motility and lipid catabolism/redistribution.

DISCUSSION

This study shows for the first time that caveolins can associate with LBs in vivo. We now show that endogenous caveolin is detectable on LBs, that the association of caveolin with LBs can be modulated, and most importantly that caveolins cannot only enter but also exit LBs by as yet unknown mechanisms. Moreover, in a physiologically relevant in vivo setting, caveolins have been demonstrated to associate with LBs, with a striking redistribution of caveolins to LBs in regenerating liver. By using a caveolin domi-

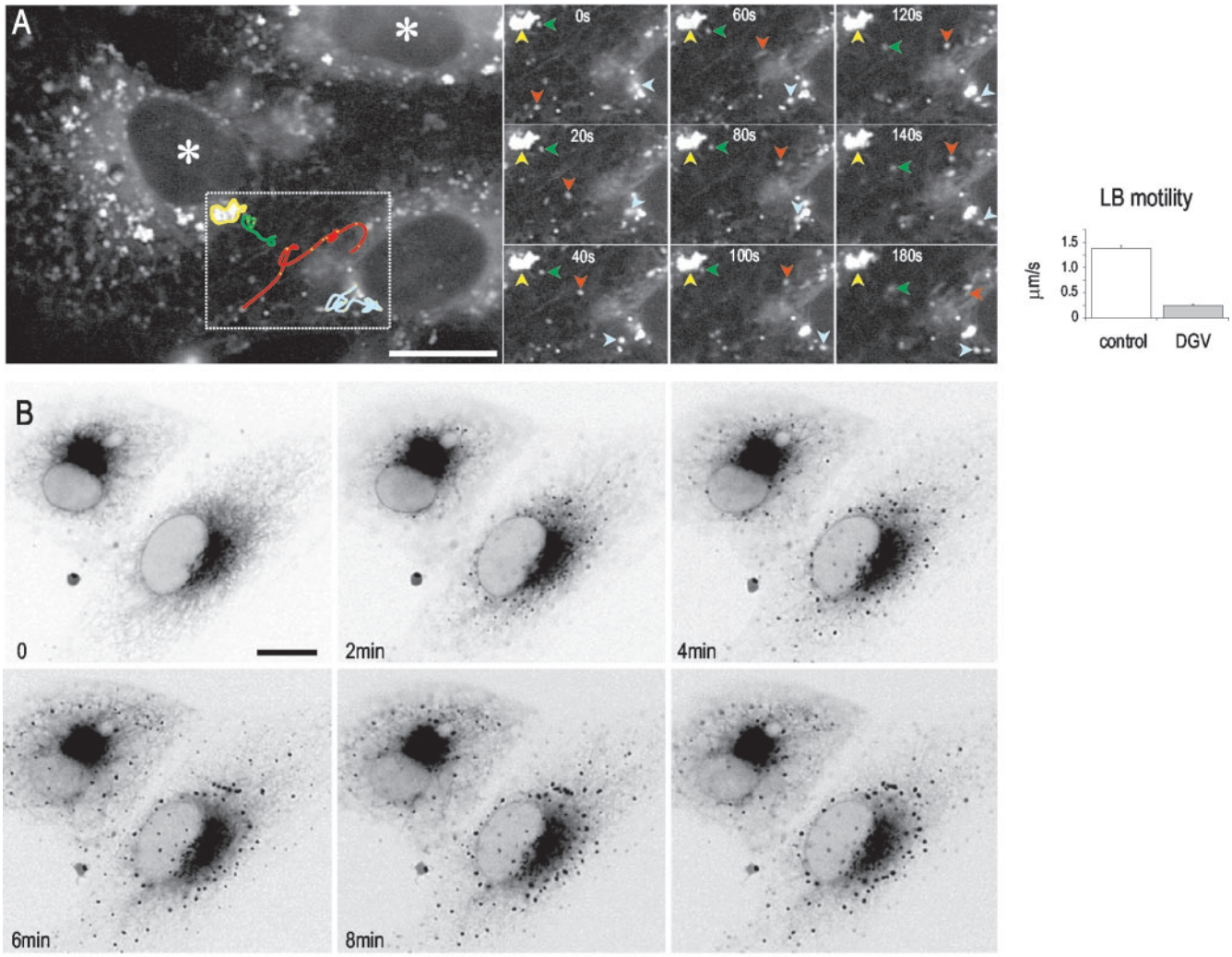

Figure 6. A caveolin dominant negative mutant affects LB motility. (A) Cav^{DGV}-GFP transfected cells were incubated in a media containing a marker for LBs, Nile red. Vero cells expressing cav^{DGV}-GFP were selected under the microscope and then observed in the Nile red channel. The field shows two cav^{DGV}-GFP–expressing cells (asterisks) and one untransfected cell. Images with a delay of 10 s were captured over 3 min. The figure shows a selected sequence of nine consecutive frames (20-s interval between images) representing a total period of 180 s. Nile red–labeled vesicles showed a rapid bidirectional saltatory movement (red, green, and blue arrows for the position in each frame or color lanes for the total trajectory). However, cav^{DGV} vesicles showed no significant motility in any axis (yellow arrows; see histogram). (B) In an attempt to study the formation of LBs containing the mutant protein, starved cells were transfected with cav^{DGV}-GFP for 24 h and then observed by videomicroscopy. Cav^{DGV} accumulated in an extensive reticular compartment identified as ER (first panel, time 0). OlAc was then added to the medium and images were captured with a constant interval of 10 s (focus was maintained at the same level). The figure shows a selected sequence of six consecutive frames representing a total period of 10 min. All the frames were processed equally and finally the image was photographically inverted to increase the contrast. In response to the lipid loading of the cell, cav^{DGV} progressively redistributes from the tubules of the ER to the forming droplets visible as distinct dots.

nant negative mutant (cav^{DGV}) we have been able to observe the remarkably rapid dynamics of LB formation. The caveolin mutant associates with LBs, causes irreversible accumulation of lipids, and inhibits their microtubule-dependent motility.

Lipid Bodies and Caveolin

The classical model for LB formation involves accumulation of lipids between the lumenal and cytoplasmic leaflets of the ER. The LBs, comprising a core of triglycerides and/or cholesterol esters, are enclosed by a single monolayer (Tauchi-Sato *et al.*, 2002). LBs are then proposed to bud away from the ER to generate free vesicles. However, a number of studies have shown that ER membranes remain in close association with the LBs (Novikoff *et al.*, 1980; Prattes *et al.*, 2000; Pol *et al.*, 2001). Rather than simply serving a storage function, a number of observations suggest a more complex role for LBs in cellular function. Signaling and trafficking proteins have been observed on the surface of lipid bodies (Yu *et al.*, 1998, 2000; Wolins *et al.*, 2001) but also see Barbero *et al.*, 2001, and the number of lipid bodies varies during the cell cycle (Gocze and Freeman, 1994).

We have previously shown that cav^{DGV}, a N-terminal truncation of cav-3, associates irreversibly to LBs and induces an intracellular cholesterol imbalance (Pol *et al.*, 2001). Because the inhibitory effects of this mutant are overcome by expression of wild-type caveolins, this raises the possibility that LBs could be part of the normal itinerary of caveolin in

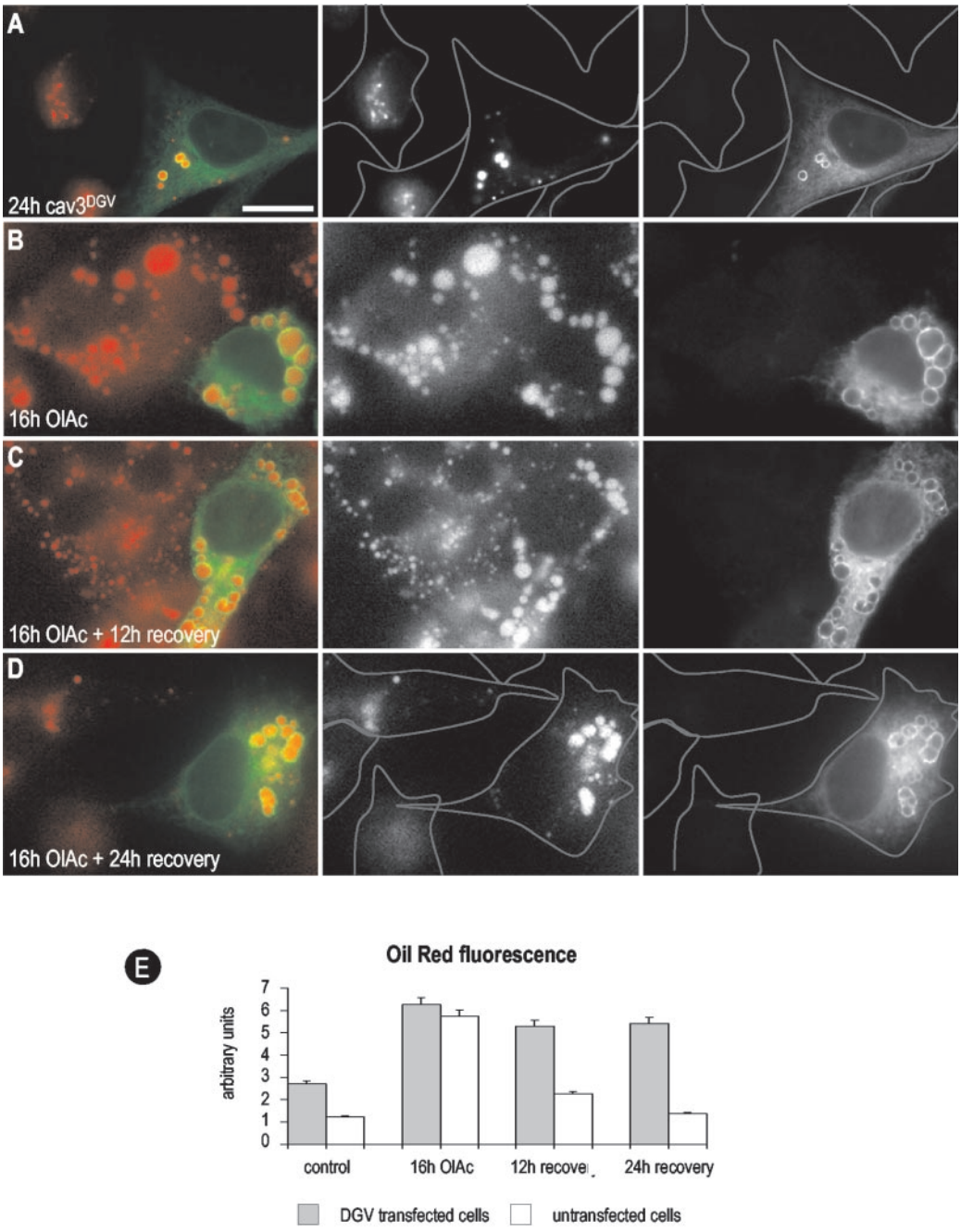

Figure 7. A caveolin dominant negative mutant inhibits lipid redistribution. (A) Cav^{DGV}-GFP was transfected in BHK cells for 24 h, the cells were fixed in PFA and stained with oil red. Cav^{DGV} induced the accumulation of LBs, but few droplets could be detected in nontransfected cells (see the profile of the cells). (B) Cav^{DGV}-GFP was transfected in BHK cells for 16 h in a medium containing OlAc. Transfected and nontransfected cells showed the accumulation of the enlarged LBs and no differences could be observed in the uptake of lipids or in the size of the droplets. (C and D) BHK cells treated as in B were incubated in a new media without OlAc. After 12 h of recovery, the LBs of nontransfected cells were greatly reduced in size. The presence of cav^{DGV} inhibited the decrease in size of the LBs and this was more apparent after 24 h. As in control cells, no LBs were observed in nontransfected cells (see profile of the cell, compare with A). In striking contrast, the OlAc induced droplets of the cav^{DGV} cells were not able to recover and kept the original size (compare D and A). Bars, 5 μm. (E) The histogram shows the quantification of the oil red–associated fluorescence in nontransfected vs. DGV transfected cells after the treatments described in A–D.

the cell. These studies prompted us to investigate the association of endogenous caveolin with LBs in cultured cells and in an in vivo situation, first as a model system to understand association of a membrane protein with LBs and second to examine whether caveolins in LBs may have some physiological role.

Taken together our results suggest that under normal culture conditions there is a relatively small pool of caveolin

associated with LBs, as judged by both biochemistry and immunofluorescence. However, in lipid-loaded cells there is a significant pool of endogenous caveolin-1 and caveolin-2 associated with LBs. This was most clearly demonstrated in FRT cells, where caveolin-2 showed oleic acid-induced translocation from the Golgi complex to LBs. Importantly, when oleic acid was removed from the culture medium, caveolin-2 redistributed back to the Golgi complex even though abundant enlarged LBs were still evident in the cells. This suggests that caveolin is not simply redistributed to LBs as a consequence of the formation of abundant enlarged LBs but that the trafficking of caveolin is regulated. It remains to be seen whether the reported fatty acid binding properties of caveolin (Trigatti *et al.,* 1999) could be involved in this process. Other proteins are known to be targeted to LBs upon oleic acid treatment including Nir2, the mammalian homologue of the *Drosophila* protein RdgB, which is associated with retinal degeneration (Litvak *et al.,* 2002). Similarly to cav^{DGV}, it has been suggested that disruption of lipid regulation by the LB-associated mutant protein might affect membrane biogenesis required for photoreceptor maintenance (Litvak *et al.,* 2002).

The long hydrophobic putative intramembrane domain of caveolin could mediate the interaction with the hydrophobic core of the LBs (Fujimoto *et al.,* 2001; Ostermeyer *et al.,* 2001). Previous studies have shown that caveolin can be cross-linked to gangliosides inserted into the extracellular leaflet of the plasma membrane (Fra *et al.,* 1995), consistent with the caveolin molecule protruding through the cytoplasmic leaflet of the LB and into the core. This model explains why caveolin, which has been compared with plant LB-associated oleosins (Brown, 2001), can associate with lipid bodies within the ER, as diffusion in the plane of the membrane would allow the preferential association of caveolin with the lipid body. However, it is much more difficult to explain the intriguing observations presented here ,which demonstrate convincingly that caveolin can exit the LB upon washout of lipids or BFA. One possibility is that mechanisms exist to decrease the affinity of caveolin for the LB core. Alternatively, interactions with other proteins might move caveolins away from the LBs, allowing their recruitment into forming transport vesicles in the ER. Both these possibilities require the LBs containing caveolin to remain ER-attached. However, LBs are generally considered to bud from the ER, and this would suggest the existence of trafficking pathways from the LBs or interactions with other organelles to explain the retrieval of caveolin from the LBs.

A Caveolin Dominant Negative Mutant Decreases LB Motility and Causes Lipid Retention in LBs

The reversible association of caveolins with LBs strengthens the hypothesis that caveolins could play some physiological role in lipid regulation. We now show that the mutant cav^{DGV} causes a dramatic decrease in the microtubule-dependent motility of LBs. Previous studies have shown that LBs exhibit bidirectional movement on microtubules and this is inhibited by disruption of the dynactin complex (Valetti *et al.,* 1999). Our studies now demonstrate that this movement can be modulated by association of the cav^{DGV} mutant. Interestingly, the mutant causes free cholesterol accumulation in late endosomes and this also inhibits late endosomal motility (Pol *et al.,* 2001), consistent with earlier studies showing Rab7-dependent motility regulation by cholesterol (Lebrand *et al.,* 2002). Second, and consistent with previous observations (Pol *et al.,* 2001), we have shown that the cav^{DGV} mutant alters neutral lipid accumulation in LBs, primarily through inhibition of neutral lipid removal from the LB stores after lipid accumulation. Accumulation of oleic acid, which is believed to diffuse across the plasma membrane and through the cytoplasm to forming LBs, is not significantly altered by the cav^{DGV} mutant. Whether the effects on LB motility and lipid removal from LBs is connected remains to be seen, but it is tempting to speculate that LB motility may facilitate movement of lipids to intracellular sites where they are required. Loss of LB motility may also contribute to the observed accumulation of free cholesterol in late endosomes. The cav^{DGV} mutant is an excellent tool to provide new insights into these processes. The results of this and our previous study (Pol *et al.,* 2001) suggest a link between the LB association of the mutant caveolin and levels of surface cholesterol as revealed by filipin staining and by functional signaling assays. In view of the complex interrelationships between the cholesterol levels in different intracellular pools it is possible that surface cholesterol levels are dependent on rates of esterification/hydrolysis in LBs. In adipocytes, removal of surface cholesterol with cyclodextrin caused mobilization of cholesterol from cholesterol ester stores in the LBs and redistribution of free cholesterol to efflux sites at the PM, suggesting an efflux pathway from LBs to the PM (Prattes *et al.,* 2000). Both pharmacological inhibition of cholesterol esterification and treatment of cells with free fatty acids has been shown to cause changes in surface free cholesterol levels (Seo *et al.,* 2002). Taken together with the results presented here, these studies suggest that LBs play a hitherto unexplored role in maintenance of surface cholesterol levels.

The cav^{DGV} mutant has also allowed us to study the formation of LBs in real time. In serum-starved cells that lack detectable LBs, the cav^{DGV} mutant accumulates in the ER. On addition of oleic acid, LBs form rapidly at discrete sites within the ER, which are spread throughout the cytoplasm. On oleic acid addition, the cav^{DGV} mutant is immediately recruited to these domains. These studies demonstrate the incredible dynamic nature of LB but also raises the question of why LBs form in specific regions of the ER. It was shown recently that the LB phospholipid composition is quite distinct to the ER, suggesting that LBs form at specific sites (Tauchi-Sato *et al.,* 2002). This provides an excellent model system to understand the exact molecular requirements for LB formation.

Caveolin Association with LBs in Regenerating Liver

Further support for the contention that the association of caveolin with LBs has physiological significance come from the findings presented here demonstrating the association of caveolin with LBs in regenerating liver After PH, there is a hormone-dependent mobilization of fat from adipose tissue (Glende and Morgan, 1968). Plasma free fatty acid levels (i.e., oleic, palmitic, palmitoleic, and linoleic acids) are five times normal levels 12–18 h after PH. As a result, the levels of hepatic cholesterol and triglycerides increase 10-fold after 18–24 h (Glende and Morgan, 1968). The steatotic (fat) liver is a paradigm, with several diseases in which the accumulation of fat in the hepatocytes has been well characterized (early stages of cirrhosis, alcoholic liver or in nonalcoholic steatotic syndromes; Koteish and Diehl, 2001).

Interestingly, during this process caveolin relocates from the PM to accumulate on LBs presumably as part of the lipid mobilization process. The reduction of caveolin/caveolae at the plasma membrane may correlate with the general arrest of endocytosis and membrane trafficking, cause a change in signaling, or is a response to the changed lipid requirements of the tissue. Caveolin has been described as a key regulator of the efflux of cellular

cholesterol. It is possible that decreasing the rate of transport of caveolin to the PM and redirecting the protein to a different compartment may result in the intracellular accumulation of cholesterol. This new pool of cholesterol could then be used for the synthesis of new membranes. Further studies are necessary to test the role that caveolin plays in the "adapted" lipid metabolism that occurs in regenerating liver. However, this is an intriguing observation that further supports the role of caveolin, now in vivo, in the intracellular homeostasis of lipids and provides new insights into the study of caveolins and LB function.

ACKNOWLEDGMENTS

This work was supported by grants from the National Health and Medical Research Council of Australia and the Human Frontiers Research Progamme to R.G.P. and grants FIS 01/1527 and G03/015 from Ministerio deSanidad y Consumo (Spain), Ministerio deCiencia y Tecnología and Fundació Maratò TV3–2001 to C.E. A.P. is supported by Ramon y Cajal Spanish Research Program (IDIBAPS). The Institute for Molecular Bioscience is a Special Research Centre of the Australian Research Council.

REFERENCES

Barbero, P., Buell, E., Zulley, S., and Pfeffer, S.R. (2001). TIP47 is not a component of lipid droplets. J. Biol. Chem. *276,* 24348–24351.

Bissell, D., Hammaker, L., and Meyer, U. (1973). Parenchymal cells from adult rat liver in nonproliferating monolayer culture. I. Functional studies. J. Cell. Biol. *59,* 722–734.

Brown, D.A. (2001). Lipid droplets: proteins floating on a pool of fat. Curr. Biol. *11,* R446–R449.

Calvo, M., Tebar, F., Lopez-Iglesias, C., and Enrich, C. (2001). Morphologic and functional characterization of caveolae in rat liver hepatocytes. Hepatology *33,* 1259–1269.

Fra, A.M., Masserini, M., Palestini, P., Sonnino, S., and Simons, K. (1995). A photo-reactive derivative of ganglioside GM1 specifically cross-links VIP21-caveolin on the cell surface. FEBS Lett. *375,* 11–14.

Franke, W.W., Hergt, M., and Grund, C. (1987). Rearrangement of the vimentin cytoskeleton during adipose conversion: formation of an intermediate filament cage around lipid globules. Cell *49,* 131–141.

Fujimoto, T., Kogo, H., Ishiguro, K., Tauchi, K., and Nomura, R. (2001). Caveolin-2 is targeted to lipid droplets, a new "membrane domain" in the cell. J. Cell Biol. *152,* 1079–1085.

Glende, E.A., Jr., and Morgan, W.S. (1968). Alteration in liver lipid and lipid fatty acid composition after partial hepatectomy in the rat. Exp. Mol. Pathol. *8,* 190–200.

Gocze, P.M., and Freeman, D.A. (1994). Factors underlying the variability of lipid droplet fluorescence in MA-10 Leydig tumor cells. Cytometry *17,* 151–158.

Greenberg, A.S., Egan, J.J., Wek, S.A., Garty, N.B., Blanchette-Mackie, E.J., and Londos, C. (1991). Perilipin, a major hormonally regulated adipocyte-specific phosphoprotein associated with the periphery of lipid storage droplets. J. Biol. Chem. *266,* 11341–11346.

Heid, H.W., Moll, R., Schwetlick, I., Rackwitz, H.R., and Keenan, T.W. (1998). Adipophilin is a specific marker of lipid accumulation in diverse cell types and diseases. Cell Tissue Res. *294,* 309–321.

Higgins, G.M., and Anderson, R.M. (1931). Experimental pathology of liver. Restoration of liver rat following partial surgical removal. Arch. Pathol. *12,* 186–202.

Koteish, A., and Diehl, A. (2001). Animal models of steatosis. Semin. Liver Dis. *21,* 89–104.

Lebrand, C., Corti, M., Goodson, H., Cosson, P., Cavalli, V., Mayran, N., Faure, J., and Gruenberg, J. (2002). Late endosome motility depends on lipids via the small GTPase Rab7. EMBO J. *21,* 1289–1300.

Litvak, V., Shaul, Y.D., Shulewitz, M., Amarilio, R., Carmon, S., and Lev, S. (2002). Targeting of Nir2 to lipid droplets is regulated by a specific threonine residue within its PI-transfer domain. Curr. Biol. *12,* 1513–1518.

Londos, C., Brasaemle, D.L., Schultz, C.J., Segrest, J.P., and Kimmel, A.R. (1999). Perilipins, ADRP, and other proteins that associate with intracellular neutral lipid droplets in animal cells. Semin. Cell Dev. Biol. *10,* 51–58.

Luetterforst, R., Stang, E., Zorzi, N., Carozzi, A., Way, M., and Parton, R.G. (1999). Molecular characterization of caveolin association with the Golgi complex: identification of a cis-Golgi targeting domain in the caveolin molecule. J. Cell Biol. *145,* 1443–1459.

Novikoff, A.B., Novikoff, P.M., Rosen, O.M., and Rubin, C.S. (1980). Organelle relationships in cultured 3T3–L1 preadipocytes. J. Cell Biol. *87,* 180–196.

Ostermeyer, A.G., Paci, J.M., Zeng, Y., Lublin, D.M., Munro, S., and Brown, D.A. (2001). Accumulation of caveolin in the endoplasmic reticulum redirects the protein to lipid storage droplets. J. Cell Biol. *152,* 1071–1078.

Parton, R.G. (1994). Ultrastructural localization of gangliosides; GM1 is concentrated in caveolae. J Histochem. Cytochem. *42,* 155–166.

Pol, A., Calvo, M., Lu, A., and Enrich, C. (1999). The early-sorting endocytic compartment of rat hepatocytes is involved in the intracellular pathway of caveolin-1 (VIP-21). Hepatology *29,* 1848–1857.

Pol, A., Luetterforst, R., Lindsay, M., Heino, S., Ikonen, E., and Parton, R.G. (2001). A caveolin dominant negative mutant associates with lipid bodies and induces intracellular cholesterol imbalance. J. Cell Biol. *152,* 1057–1070.

Prattes, S., Horl, G., Hammer, A., Blaschitz, A., Graier, W.F., Sattler, W., Zechner, R., and Steyrer, E. (2000). Intracellular distribution and mobilization of unesterified cholesterol in adipocytes: triglyceride droplets are surrounded by cholesterol-rich ER-like surface layer structures. J. Cell Sci. *113,* 2977–2989.

Qu, R.D., and Huang, A.H. (1990). Oleosin KD 18 on the surface of oil bodies in maize. Genomic and cDNA sequences and the deduced protein structure. J. Biol. Chem. *265,* 2238–2243.

Seo, T., Velez-Carrasco, W., Qi, K., Hall, M., Worgall, T.S., Johnson, R.A., and Deckelbaum, R.J. (2002). Selective uptake from LDL is stimulated by unsaturated fatty acids and modulated by cholesterol content in the plasma membrane: role of plasma membrane composition in regulating non-SR-BI-mediated selective lipid transfer. Biochemistry *41,* 7885–7894.

Tauchi-Sato, K., Ozeki, S., Houjou, T., Taguchi, R., and Fujimoto, T. (2002). The surface of lipid droplets is a phospholipid monolayer with a unique fatty acid composition. J. Biol. Chem. *277,* 44507–44512.

Trigatti, B.L., Anderson, R.G., and Gerber, G.E. (1999). Identification of caveolin-1 as a fatty acid binding protein. Biochem. Biophys. Res. Commun. *255,* 34–39.

Uittenbogaard, A., Everson, W.V., Matveev, S.V., and Smart, E.J. (2002). Cholesteryl ester is transported from caveolae to internal membranes as part of a caveolin-annexin II lipid-protein complex. J. Biol. Chem. *277,* 4925–4931.

Uittenbogaard, A., Ying, Y., and Smart, E.J. (1998). Characterization of a cytosolic heat-shock protein-caveolin chaperone complex. Involvement in cholesterol trafficking. J. Biol. Chem. *273,* 6525–6532.

Valetti, C., Wetzel, D.M., Schrader, M., Hasbani, M.J., Gill, S.R., Kreis, T.E., and Schroer, T.A. (1999). Role of dynactin in endocytic traffic: effects of dynamitin overexpression and colocalization with CLIP-170. Mol. Biol. Cell. *10,* 4107–4120.

van Meer, G. (2001). Caveolin, cholesterol, and lipid droplets? J. Cell Biol. *152,* F29–F34.

Wang, S.M., and Fong, T.H. (1995). A lipid droplet-specific capsule is present in rat adrenal cells: evidence from a monoclonal antibody. Biochem. Biophys. Res. Commun. *217,* 81–88.

Weller, P.F., and Dvorak, A.M. (1994). Lipid bodies: intracellular sites for eicosanoid formation. J. Allergy Clin. Immunol. *94,* 1151–1156.

Wolins, N.E., Rubin, B., and Brasaemle, D.L. (2001). TIP47 associates with lipid droplets. J. Biol. Chem. *16*(276(7)), 5101–5108.

Yu, W., Bozza, P.T., Tzizik, D.M., Gray, J.P., Cassara, J., Dvorak, A.M., and Weller, P.F. (1998). Co-compartmentalization of MAP kinases and cytosolic phospholipase A2 at cytoplasmic arachidonate-rich lipid bodies. Am. J. Pathol. *152,* 759–769.

Yu, W., Cassara, J., and Weller, P.F. (2000). Phosphatidylinositide 3-kinase localizes to cytoplasmic lipid bodies in human polymorphonuclear leukocytes and other myeloid-derived cells. Blood *95,* 1078–1085.